Differential Emission Measure Reconstruction with the Atmospheric Imaging Assembly

M.A. Weber, E.E. DeLuca, L. Golub, and A.L. Sette
Harvard-Smithsonian Center for Astrophysics, 60 Garden Street, Cambridge, MA 02138
`mweber@cfa.harvard.edu, edeluca@cfa.harvard.edu, golub@cfa.harvard.edu, asette@cfa.harvard.edu`

Poster ID: Magnetic Field Topology & Solar Dynamics — 4.23P

ABSTRACT

The Atmospheric Imaging Assembly (AIA) will be one of the instruments on the Solar Dynamics Observatory (SDO). It will image the solar transition region and corona in multiple EUV and UV wavelengths simultaneously, using four aligned telescopes. Hence, AIA will be capable of high-cadence, spatially-resolved temperature discrimination of solar plasmas. We investigate a method for using AIA observations to produce differential emission measure (DEM) reconstructions. We find that the number of observation channels and the solution temperature range significantly impact the quality of temperature and DEM analysis with a normal-incidence, narrowband imager like AIA. We also consider the effects of random and systematic errors.

1. TEMPERATURE DISCRIMINATION WITH AIA

Two of the main considerations in the design of AIA are temperature (T) coverage and temperature discrimination. In order to meet the instrument's scientific objectives by the observation of the solar corona, AIA must be able to distinguish plasma structures for 0.7 MK $< T <$ 20 MK, i.e., determine DEM(T). For this purpose, AIA uses six narrowband EUV channels selected carefully for coronal ion lines and complete coverage in this T range (see Fig. 1).

As pointed out many years ago (Craig & Brown, 1976), there are limitations to the ability to determine a source temperature distribution of a hot plasma by spectroscopic means. The main limitation is a fundamental one: the flatness of the emission kernel due to the Boltzmann width $e^{-\epsilon/kT}$. This makes the spectrum relatively insensitive to the DEM, and makes the inversion problem poorly-determinable. However, AIA will have an advantage over previous solar imagers in the number of nearly simultaneous coronal EUV channels (6), rapid cadence (Δt = 10s), and high spatial resolution (1.2 arc-seconds) which will likely provide views of more nearly isothermal plasma.

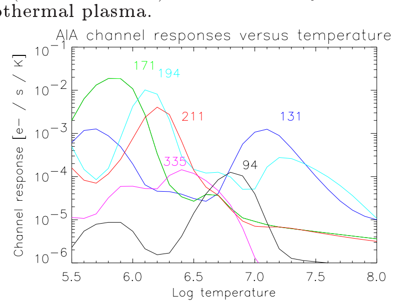

Figure 1: AIA EUV channel temperature responses. Each channel is labeled by its characteristic wavelength (Ångstroms). These responses assume a DEM(T) = 10^{22} cm^{-5} K^{-1}.

2. ITERATIVE FORWARD MODELING OF DEMs

We consider a set of AIA images taken of an active region (AR), using the primary EUV channels (see Fig. 1). We assume that the structure of the AR loops is unchanged during the time it takes for AIA to accumulate all of the images. Before processing, the set of AIA images is co-aligned and reduced to physical units (e.g., DN/s). In this section, we discuss how we estimate the DEM in a given pixel.

Our procedure produces an iterative least-squares fit to the observations using a DEM represented by a spline with evenly spaced knots in log(T_e) space. For the set of observations (all c) in pixel i, we solve the simultaneous equations

$$O_{ic} = \int Q_i(T)\, I_c(T)\, \mathrm{d}T, \qquad (1)$$

where O_{ic} is the observation of the i-th pixel in spectral channel c, $Q_i(T)$ is the differential emission in the i-th pixel, and $I_c(T)$ is the instrumental response function for channel c for a differential emission measure that is constant in T. With the forward modeling approach, we assume a DEM, apply Eq. (1), and compare the predicted observations for each filter with the real observations. The optimal DEM spline is found by IDL `mpfit` routines from Craig B. Markwardt (`http://cow.physics.wisc.edu/~craigm/idl/idl.html`), using a non-linear least-squares method.

A basic problem with the forward modeling approach is determining the relevance of the best-fit solution. The AIA EUV-wavelength response functions are narrow in wavelength, but broad in temperature coverage with significant overlap (Fig. 1). There is the possibility of finding multiple solutions to the observations which correspond to substantially different DEM(T) curves. To address this issue we expand our nominal set of observations into 100 different Monte Carlo (M.C.) realizations by adding random noise, consistent with the photon noise (typically 3%), to the observations. The best least-squares fit to each of the realizations is then determined as the median fit per temperature bin. Our confidence in the fit is measured by the fluctuations in the fits about the median.

3. SINGLE TEMPERATURE DEMs

Figs. 2 indicate AIA's ability for temperature determination. Our DEM reconstruction method is able to accurately identify the temperature of isothermal plasma, throughout AIA's effective temperature range. Since our method uses DEM splines, there is inherent difficulty fitting these sharp functions. This explains the "leakage" to adjacent T bins.

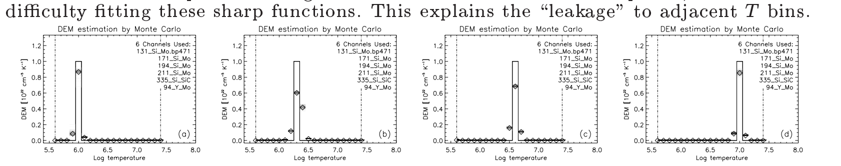

Figure 2: Reconstruction of single-T DEMs. The solid lines indicate the DEM models which the method is attempting to reconstruct. These DEM models have a value of 10^{22} cm^{-5} K^{-1} for log T bin = (a) 6.0, (b) 6.3, (c) 6.6, and (d) 7.0, respectively, and are zero elsewhere. The M.C. distribution of 100 solutions for 3% noise is represented by grayscale shading. The median solutions are indicated by diamonds. The vertical dashed lines mark the temperature range over which the DEM is reconstructed.

4. THE VALUE OF MANY CHANNELS

The corona is known to be highly inhomogeneous in temperature, density, and magnetic field— the isothermal approximation may be inadequate for describing the optically thin solar atmosphere across length scales comparable to the span of an AIA pixel. We consider a DEM model for an active region, derived from solar observations (Dupree et al., 1973). Fig. 3a shows a "best-fit", using all six EUV coronal channels. Figs. 3b and 3c show the minimum and maximum effect of using just five channels. Fig. 3d shows the effect using just four channels. All six channels are necessary to get an accurate DEM reconstruction.

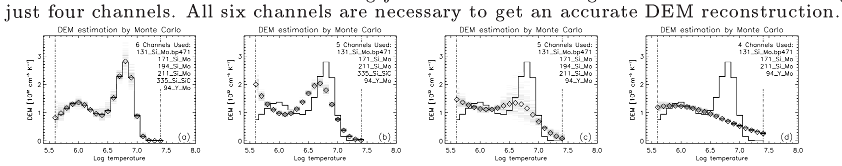

Figure 3: Number of channels for DEM reconstruction. (a) All six EUV coronal channels; (b) not using 194Å; (c) not using 335Å; and (d) not using 194Å and 335Å. Plotting scheme same as for Fig. 2.

5. THE EFFECTS OF TEMPERATURE RANGE

The selection of observation channels has implications for the temperature range over which DEM(T) can be accurately reconstructed. We find that the reconstruction method is sensitive to the assumed T-range. Fig. 3a indicates that the AR DEM model is best reconstructed with the six AIA channels over the range log T = 5.6–7.4. Figs. 4a, 4b display the results of varying the low end of this T range. Figs. 4c, 4d display the results varying the high end.

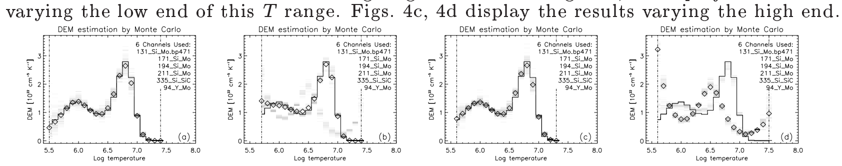

Figure 4: Effects of assumed temperature range. The assumed T-range for the DEM reconstruction is (a) 5.5–7.4; (b) 5.7–7.4; (c) 5.6–7.3; and (d) 5.6–7.5. Plotting scheme same as for Fig. 2.

6. RANDOM & SYSTEMATIC ERRORS

We investigated the effects of random and systematic errors on the quality of DEM reconstruction by this method. Fig. 5a shows a typical DEM reconstruction with the effect of 3% noise reflected in the span of solutions.

The effects of random errors. The M.C. distributions in each temperature bin are virtually symmetric and are well-fitted by Gaussians. We fit σ_{DEM} in each temperature bin such that (median $\pm\ \sigma_{\mathrm{DEM}}$) included the central 68% of the M.C. realizations. We investigated the behavior of σ_{DEM} versus the level of random noise (1%, 3%, 10%, 30%). Our results (not shown here) indicate that σ_{DEM} increases proportionally with noise. The level of random noise does not appreciably affect the median estimate of the DEM.

The significance of systematic errors. Fig. 5b is produced from Fig. 5a by subtracting the DEM model. In other words, we have plotted the residuals of our median estimate relative to the model, including the 1-σ_{DEM} error bars. The full χ^2 value is given. We calculate a related statistic ($\overline{r_{\mathrm{DEM}}}$), which is the mean residual per temperature bin in units of standard deviations.

$$\overline{r_{\mathrm{DEM}}} = \sqrt{\chi^2/N_T} = \sqrt{\sum_{j=1}^{N_T} (\mathrm{DEM}_j - \mathrm{DEM}_{\mathrm{model}})^2/(\sigma_j^2 N_T)}. \qquad (2)$$

To evaluate systematic error, constant offsets were applied to one channel for sets of M.C. realizations with 3% noise. Fig. 5c plots $\overline{r_{\mathrm{DEM}}}$ versus the level of systematic error applied to the 171A channel. This plot indicates that a 10% systematic error on top of 3% random error permits accuracy in DEM reconstruction at the 2.5-σ level.

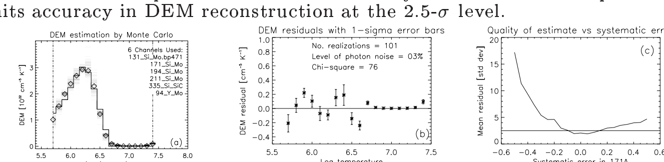

Figure 5: Impact of systematic errors. (a) Reconstruction for an arbitrary "active region-like" DEM, with 3% noise. (b) Residuals for Fig. 5a. (c) Mean residual (in standard deviations) versus systematic error applied to the 171Å channel.

REFERENCES & ACKNOWLEDGEMENTS

Dupree, A.K., et al. 1973, *ApJ*, **182**, 321
Craig, I.J.D., & Brown, J.C. 1976, *A&A*, **49**, 239
This work supported under AIA contract SP02D4301R with Lockheed Martin Corp.